The triangle of ageing: a model of how repair, resilience to damage and asymmetric segregation are responses to replicative ageing

Johannes Borgqvist[1], Niek Welkenhuysen[1], Marija Cvijovic[1*]

1 Department of Mathematical Sciences, Chalmers University of Technology and the University of Gothenburg, Gothenburg, Sweden.

*Corresponding Author: Marija Cvijovic, Phone: +46 31 772 53 21, e-mail: marija.cvijovic@chalmers.se

Abstract

Accumulation of damaged proteins is a hallmark of ageing occurring in organisms ranging from bacteria and yeast to mammalian cells. During cell division in *Saccharomyces cerevisiae*, damaged proteins are retained within the mother cell. This results in a new daughter cell with full replicative potential and an ageing mother with a reduced replicative lifespan (RLS). The cell-specific features determining the lifespan remain elusive. It has been suggested that the RLS is dependent on the ability of the cell to repair and retain pre-existing damage. To deepen the understanding of how these factors influence the life span of individual cells, we developed a dynamic model of damage accumulation accounting for replicative ageing. The model includes five essential properties: cell growth, damage formation, damage repair, cell division and cell death. Based on these, we derive the triangle of ageing: a complete theoretical framework describing the conditions allowing for replicative ageing, starvation, immortality or clonal senescence. Exploiting this framework, we propose that the retention mechanism is fundamental for ageing. Furthermore, we suggest that resilience to damage is a central trait influencing replicative ageing which can be used as a basis for life prolonging strategies. In addition, the model is in agreement with experimental data consisting of RLS distributions and mean generation times from three yeast strains: the short lived *sir2*Δ, the wild type *wt* and the long lived *fob1*Δ. This validates the underlying assumptions and we conclude that strains with an efficient repair machinery require retention. Finally, the triangle of ageing suggests that asymmetric cell division is beneficial with respect to replicative ageing as it increases the RLS of a given organism. Thus, the proposed model indicates that in order to obtain a mechanistic understanding of the ageing process in eukaryotic organisms it is critical to investigate the constituents of the retention machinery.

Author summary

Cells age by accumulating damage over time. In budding yeast, damage is inherited asymmetrically such that most is retained within the mother cell. Nevertheless the nature and the interplay behind the driving forces of this process remain unknown. In this study, we develop a single cell model of accumulation of damage accounting for replicative ageing that includes five key properties: cell growth, formation of damage, repair of damage, cell division and cell death. Using mathematical analysis of the model,

we derive the *triangle of ageing*, a theoretical framework identifying damage retention as a key factor underlying ageing in yeast. This model represents an important step in elucidating the mechanisms behind damage segregation and can be valuable for understanding similar phenomena in other organisms.

Introduction

Cell division, growth and death are fundamental features of any living organism. During its life cycle, a cell produces a set of functional components, proteins or other metabolites, which will ultimately allow the cell to divide giving rise to a newly born daughter cell. However, due to inherent imperfections in the cellular machinery over time, cells are slowly deteriorating causing essential intracellular functions to perish. At the very end of a cell's lifespan, age-associated damage builds up consistently impairing the ability of the cell to divide and survive which eventually culminates in cell death. In environments with a sufficient amount of food, damage will be formed as a consequence of cell growth. This causes the partitioning of damage between progenitor and progeny during cell division to be an important function.

An asymmetric distribution of cell mass after division constitutes a vital part of ageing in the yeast *Saccharomyces cerevisiae* (*S.cerevisiae*). The number of divisions before cell death is a measure of the age of a single yeast cell which has been studied substantially by means of experiments [1, 2, 3], and it is called the replicative life span (RLS). The asymmetric division of the budding yeast results in a large ageing mother cell with a finite RLS and a new small daughter cell with full replicative potential [4]. Replicative ageing in yeast is characterised by the accumulation of age-related damage that is selectively retained within the mother cell compartment at each division [5]. This retention of damage is required to rejuvenate daughter cells and thereby maintain viability in populations over time. The described mode of division resembles the division observed in multicellular organisms characterised by the separation of the soma and the germ cell lines [6]. However, the details behind the interaction of the involved systems and their effects on ageing are still largely unknown. To elucidate the interplay between the various constituents of these processes, theoretical approaches are often implemented in addition to experimental methods.

Hitherto, multiple qualitative mathematical models of the accumulation of damage have been developed [7, 8, 9, 10, 11, 12, 13]. One of the first models showed that even simple unicellular bacteria undergo ageing as a means to cope with damage [7]. This finding suggested that the phenomenon of ageing precedes eukaryotes and has evolved numerous times as it occurs in multiple organisms. A model of damage accumulation showed the importance of asymmetric partitioning of damage through retention in the symmetrically dividing fission yeast *Schizosaccharomyces pombe* (*S.pombe*) and in the asymmetric budding yeast *S.cerevisiae* as it increases the fitness of the population at both low and high damage propagation rates [8]. A model of ageing in the bacteria *Escherichia coli* (*E.coli*) showed that under the examined conditions the cell lineage was immortal due to its low rate of formation of damage [9]. A follow-up model quantified the importance of a deterministic (as opposed to a stochastic) asymmetric distribution of damage upon cell division [12], also concluding that asymmetric partitioning of damage increases the overall fitness of the population. An additional study in yeast proposed that the ratio between maintenance and growth is critical when determining the benefits of symmetric and asymmetric division [10]. Furthermore, damage repair has been identified as a better strategy in terms of coping with damage compared to asymmetric segregation [11]. Most recently, it was demonstrated that asymmetric segregation of damage in *E.coli* is deleterious for the individual cell, but it is beneficial for the population as a whole [13]. In general, these models include the five key properties *cell growth*, *formation*

of damage, *repair of damage*, *cell division* and *cell death* to a varying extent. Further, a commonly implemented methodology consists of conducting simulations in order to draw conclusions about the effects of the accumulation of damage on a population level.

Provided the current models, two main shortcomings should be addressed, namely the population level focus and the choice of mainly using simulations as a methodology. The availability of single cell level data with regards to replicative ageing [14] allows us to shift the focus from population level properties which render the models hard to validate by experimental data. Further, as the dynamical properties of the models are not analysed it is hard to verify whether the models are reasonable or not with respect to the cellular properties they describe. Also, mathematical analysis opens the possibility to draw general conclusions about numerous properties of replicative ageing and to determine the allowed parameters that give rise to reasonable RLSs. In addition, this methodology can also simplify the task of finding parameters that can otherwise be hard to estimate. To our knowledge, the usage of thorough mathematical analysis in combination with simulations coupled to single cell data of replicative lifespans in order to obtain a detailed description of the constituent parts has not been performed. Moreover, the synergistic effects of the formation of damage, repair of damage and retention are unknown as well as the conditions allowing cells to invest in various strategies such as prioritising retention over repair.

Here we address these questions by creating a comprehensive replicative ageing model on the single cell level. The model which includes all five key properties is verified by available RLS measurements and generation times of individual cells. The implemented mathematical analysis provides a deep understanding of the interplay between the fundamental constituent forces such as damage formation, repair and retention summarised in a framework termed the *triangle of ageing*. This framework describes the conditions determining if a given cell will undergo replicative ageing, starvation, immortality or clonal senescence. Also, the triangle of ageing allows us to examine ways of altering the rate of repair and formation of damage as strategies to increase the age tolerance of a single cell. We found that the retention mechanism is a fundamental force behind replicative ageing as it increases the range of cells that undergo ageing and it enables a high RLS. Further, we determine that long-lived yeast strains have an effective repair machinery relative to their damage formation rate on account of their functioning retention mechanism. Finally, we show the evolutionary benefit of asymmetric cell division and high damage resilience in the context of replicative ageing.

Results

The replicative ageing model

To investigate the interplay between the key properties underlying the replicative ageing of individual cells, we have developed a dynamic model of damage accumulation. In the model, a cell is assumed to contain two components: intact proteins and damage consisting of malfunctioning proteins. The model includes five essential properties: cell growth, formation of damage, repair of damage, cell division, and cell death (Fig 1B). Cell division and cell death are modelled as discrete events, while the dynamics of intact proteins (P) and damaged proteins (D) is continuous. The continuous part, which is described by a coupled system of *ordinary differential equation*s (ODEs) (Eq (1)), is

governed by cell growth, formation of damage, and repair of damage.

$$\begin{aligned}\frac{\mathrm{d}P}{\mathrm{d}t} &= \overbrace{\mu\left(S\right)P\left(g-\frac{D}{D_{\mathrm{death}}}\right)}^{\text{Cell growth}} - \overbrace{k_1 P}^{\substack{\text{Damage}\\ \text{Formation}}} + \overbrace{k_2 D}^{\text{Repair}} \\ \frac{\mathrm{d}D}{\mathrm{d}t} &= k_1 P - k_2 D \end{aligned} \tag{1}$$

$$\begin{aligned} P(0) &= f_P\left(s,\mathrm{re}\right), \quad D\in[0,D_{\mathrm{death}}],\ P\in[0,P_{\mathrm{div}}] \\ D(0) &= f_D\left(s,\mathrm{re}\right), \quad t\in\mathbb{R}_+, \quad g\in(1,\infty), \quad k_1,k_2\in\mathbb{R}_+ \end{aligned}$$

Cell growth: The cell growth is dictated by the availability of key nutrients, such as sugars, amino acids, and nitrogen compounds [15]. In the model, the growth of the cell is assumed to be exponential: "$\mu\left(S\right)\cdot P$". The rate $\mu\left(S\right)=\mu_{\max}\frac{S}{K_S+S}$ is modelled by Monod growth [11, 16] where $\mu_{\max}\ \left[\mathrm{h}^{-1}\right]$ is the specific growth rate, K_S [M] is the Monod constant and S [M] is the substrate concentration. An abundance of substrate is assumed to be available for each cell ($S=S_{\mathrm{in}}$) as would occur in a microfluidics system with continuous inflow of nutrient rich media (Fig 1A) [17, 18]. As the rate of cell growth declines with increasing amounts of damage [19, 3] the unit-less factor $\left(g-\frac{D}{D_{\mathrm{death}}}\right)$ is included in the growth term. The parameter g is a positive number that is larger than 1 and determines the decline in growth rate. Thus, as D approaches the death threshold D_{death} the difference $\left(g-\frac{D}{D_{\mathrm{death}}}\right)$ will decrease corresponding to a slower growth rate.

Damage formation: As a consequence of cell growth damage is formed. The various types of ageing related damage are called ageing factors or ageing determinants. They are comprised of cell compounds or cellular organelles whose functional decline over time results in a toxic effect [20, 21, 22]. In the model, we focus on damaged proteins as the ageing factor of interest. These are formed by either newly synthesised proteins that are not correctly folded or functional proteins that become unfolded. In the model, a constant proportion of the existing intact proteins P is converted to the reversible damage D with the damage formation rate $k_1\ \left[h^{-1}\right]$.

Damage repair: Since damaged proteins have a deleterious effect, the cell has developed several strategies to eliminate them. Damaged proteins are sorted for either repair to their proper state mediated by molecular chaperones or to degradation through the targeting of the damaged proteins to the ubiquitin-proteasome system. The system acts by moving damaged proteins into specific protein inclusions before being degraded or refolded [23, 24, 25]. In the model, we consider repair as a strategy for the cell to remove accumulated damage. A constant proportion of the existing damaged proteins D is converted to intact proteins P with the damage repair rate $k_2\ \left[h^{-1}\right]$.

Cell death: Cell death constitutes an important part of the process of ageing [26, 27, 28]. Cells that have reached their full RLS potential show signs of programmed cell death [27]. How the gradual deterioration over time associated with ageing ultimately leads to cell death is unknown [28]. Here, we assume that damaged proteins are deleterious for the cell and therefore cell death occurs when the amount of damaged proteins D reaches the death threshold D_{death}. When this critical amount of damage is reached, the cell stops growing and is removed from the simulation.

Cell division: Cell division occurs when the cell reaches a certain size. During division in *S. cerevisiae*, damaged proteins are actively retained in the mother cell [5, 21, 25]. This asymmetric segregation of damage is required to rejuvenate daughter cells and to maintain viability in populations over time. In the model, we assume that the size

of a cell is proportional to the build-up of key proteins and that a cell divides when the amount of intact proteins P reaches the division threshold P_{div}. Upon cell division, the intact and damaged proteins are distributed between the mother and daughter cell. This event is controlled by two parameters: the size proportion s and the retention value re. The size proportion $s \in \left[\frac{1}{2}, 1\right)$ corresponds to the size of the mother cell and $(1-s)$ corresponds to the size of the daughter cell. The size proportion in the fission yeast *S.pombe* or *E.coli* is $s = \frac{1}{2}$ and corresponds to symmetric cell division. The bakers yeast *S.cerevisiae* divides asymmetrically with $s = \frac{3}{4}$ [29]. The retention value re $\in [0, 1]$ corresponds to the proportion of damage that is retained in the mother cell after cell division where the value re $= 1$ corresponds to *all* damage being retained while no retention is given by re $= 0$. The distribution of intracellular components after cell division is based on the principle of *mass conservation* over generations (Eq (2)) [8]. This means that the total cellular content, that is $(P + D)$, of the original cell before division equals the sum of the total cellular content of the mother and daughter cell after division. The conditions are also based on mass conservation with respect to intact proteins P and damage D. The initial amounts of intact proteins and damage in a cell after cell division are determined by the functions f_P and f_D, respectively.

$$
\begin{aligned}
f_P\,(s, \text{re}) &= \begin{cases} s\,P_{\text{div}} - \text{re}(1-s)D & \text{[Mother]} \\ (1-s)\,P_{\text{div}} + \text{re}(1-s)D & \text{[Daughter]} \end{cases} \\
f_D\,(s, \text{re}) &= \begin{cases} (s + (1-s)\text{re})\,D & \text{[Mother]} \\ (1-s)(1-\text{re})D & \text{[Daughter]} \end{cases}
\end{aligned}
\tag{2}
$$

Figure 1. Schematic representation of the model. **(A)** The cultivation of cells in a dynamic setting such as a microfluidics device. The inflow of substrate in the dynamic setting is denoted S_{in} and the amount of substrate available for the cells is denoted S. **(B)** The dynamics of a single cell. The production of intact proteins (blue squares) and damage (brown circles) is determined by the processes cell growth, formation and repair of damage. When $P = P_{\text{div}}$ cell division occurs, and the distribution of components between the mother and daughter cell is determined by the functions f_P and f_D. When $D = D_{\text{death}}$ cell death occurs. **(C)** The effect of the damage resilience parameter $Q = \left({}^{D_{\text{death}}}/_{P_{\text{div}}}\right)$ on the RLS of single cells. The cell divisions are followed over time for three single cells with low $\left[\text{blue graph} : \left(Q = {}^{1}/_{3}, \text{RLS} = 6\right)\right]$, medium $\left[\text{red graph} : \left(Q = {}^{2}/_{5}, \text{RLS} = 9\right)\right]$ and high $\left[\text{green graph} : \left(Q = {}^{1}/_{2}, \text{RLS} = 21\right)\right]$ resilience to damage. The length of the ''steps" of the stairs represents the generation time. The other parameters used in the simulations are $\mu(S) = 0.6$, $g = 1.4$, $k_1 = 0.1$, $k_2 = 0.145$, $s = {}^{3}/_{4}$, $(P_0, D_0) = (1-s, 0)$ and re $= 0.875$.

To account for the individuality of each cell, the rate parameters (k_1, k_2) are drawn from a log-normal probability distribution (Eq (3)) [30, 31]. In similarity with Mixed Effect Modelling, the individual parameters (k_1, k_2) of each cell depend on fixed effects and mixed effects [32, 33]. The fixed effects for both parameters are denoted with a bar, i.e. $\left(\overline{k_1}, \overline{k_2}\right)$, and these are constant for each population. The mixed effects (η_1, η_2) which vary between individuals within the population are two normally distributed variables with zero mean and variances $(\sigma_{k_1}, \sigma_{k_2})$.

$$
\begin{aligned}
k_1 &= \overline{k_1} \cdot e^{\eta_1}, \quad \eta_1 \sim \mathcal{N}\left(0, \sigma_{k_1}\right) \\
k_2 &= \overline{k_2} \cdot e^{\eta_2}, \quad \eta_2 \sim \mathcal{N}\left(0, \sigma_{k_2}\right)
\end{aligned}
\tag{3}
$$

Non-dimensionalisation introduces the property of resilience to damage

To by-pass the estimation of the parameters which can not be measured and to scale down the number of parameters, we non-dimensionalise the model. To this end, all the states and the time variable are scaled in a way such that the variable, states, and parameters of the resulting model lacks physical dimensions. This in turn simplifies the comparison between the various model components (see Supplementary material S2.1). The states P and D are typically measured in molars [M] as well as their corresponding threshold values P_{div} and D_{death}. Since both upper thresholds of the intact and damaged proteins are hard to estimate, we introduce the dimensionless states $P, D \in [0, 1]$ by scaling each state with its respective threshold: $P \leftarrow \left({}^{P}/_{P_{\text{div}}}\right)$ and $D \leftarrow \left({}^{D}/_{D_{\text{death}}}\right)$. The introduction of these new states which are proportions of their respective thresholds results in the removal of the two threshold values P_{div} and D_{death} from the model. Similarly, the time t measured in hours [h] is non-dimensionalised by introducing the variable τ defined as $\tau = \mu_{\max} \cdot t$. A summary of all the dimensionless components of the model is presented in Tab 1. After the non-dimensionalisation, the continuous (Eq (1)) and discrete (Eq (2)) part of the model are given by Eq (4) and (5), respectively.

Dynamics of intact and damaged proteins:

$$\begin{aligned} \frac{\mathrm{d}P}{\mathrm{d}\tau} &= \mu\left(S\right) P \left(g - D\right) - k_1 P + k_2 Q D \\ \frac{\mathrm{d}D}{\mathrm{d}\tau} &= \frac{k_1}{Q} P - k_2 D \end{aligned} \tag{4}$$

$$\begin{aligned} P(0) &= f_P\left(s, \mathrm{re}\right), \quad D, P \in [0,1], \quad \tau \in \mathbb{R}_+ \\ D(0) &= f_D\left(s, \mathrm{re}\right), \quad t \in \mathbb{R}_+, \quad g \in (1, \infty) \quad k_1, k_2 \in \mathbb{R}_+, \quad Q \in (0, 1] \end{aligned}$$

Cell division:

$$\begin{aligned} f_P\left(s, \mathrm{re}\right) &= \begin{cases} s - \mathrm{re}(1-s)QD & \text{[Mother]} \\ (1-s) + \mathrm{re}(1-s)QD & \text{[Daughter]} \end{cases} \\ f_D\left(s, \mathrm{re}\right) &= \begin{cases} \left(s + (1-s)\mathrm{re}\right) D & \text{[Mother]} \\ (1-s)(1-\mathrm{re})D & \text{[Daugther]} \end{cases} \end{aligned} \tag{5}$$

Non-dimensionalisation introduces the parameter Q termed the *damage resilience parameter*. It is defined as the quotient between the death and division thresholds, i.e. $Q = \frac{D_{\text{death}}}{P_{\text{div}}}$, and can be interpreted as the capacity of the cell to cope with damage. A high value of Q is close to 1, as it is assumed $D_{\text{death}} \leq P_{\text{div}}$, which corresponds to an organism that is resilient to damage. To test the effect of this parameter on the RLS, we have followed the number cell divisions over time for three individual cells with low, medium and high resilience to damage. As expected, an increase in the resilience to damage of a single cell yields a higher RLS (Fig 1C) and increases the average generation time: $\overline{\tau}\left(Q = {}^{1}/_{3}\right) = 0.86$, $\overline{\tau}\left(Q = {}^{2}/_{5}\right) = 0.8935$ and $\overline{\tau}\left(Q = {}^{1}/_{2}\right) = 1.1263$ (See Supplementary Material S1.3).

All dimensionless parameters can be estimated except for the *damage formation rate* k_1 and the *repair rate* k_2 (See Supplementary Material S1.2). Therefore, it is of particular interest to pick parameter pairs (k_1, k_2) that give rise to biologically reasonable

dynamics. In order to achieve this goal, it is possible to constrain the parameter space by analysing the mathematical properties of the model at hand.

Table 1. The dimensionless components of the models. All the states, variable and parameters of the model are listed in the left column and their descriptions are provided in the right column.

Component	Description
$P \leftarrow \frac{P}{P_{\text{div}}}$	The proportion of intact proteins is one of the two states of the model. It lies in the interval $P \in [0,1]$ and $P = 1$ results in cell division.
$D \leftarrow \frac{D}{D_{\text{death}}}$	The proportion of damage is one of the two states of the model. It lies in the interval $D \in [0,1]$ and $D = 1$ results in cell death.
$\tau = \mu_{\max} \cdot t$	The dimensionless time variable of the model is given by the time scaled by the specific uptake rate $\mu_{\max}$.
$\mu(S) \leftarrow \frac{S}{K_S+S}$	The cell growth factor depending on the dimensionless substrate S and the dimensionless Monod coefficient K_S.
$S \leftarrow \frac{S}{S_{\text{in}}}$	The dimensionless substrate $S \in [0,1]$ as a proportion of the inflow of substrate S_{in} to the system. The value $S = 1$ corresponds to a cell having full availability of substrate.
$K_S \leftarrow \frac{K_S}{S_{\text{in}}}$	The dimensionless Monod coefficient as a proportion of the inflow of substrate S_{in} to the system.
g	A cell growth factor. It is included in the non-linear growth term "$\mu(S)\,P\,(g - D)$" ensuring a declining rate of cell growth with age.
$k_1 \leftarrow \frac{k_1}{\mu_{\max}}$	The damage formation rate as a proportion of the specific growth rate $\mu_{\max}$.
$k_2 \leftarrow \frac{k_2}{\mu_{\max}}$	The damage repair rate as a proportion of the specific growth rate $\mu_{\max}$.
$Q = \frac{D_{\text{death}}}{P_{\text{div}}}$	The damage resilience parameter corresponding to the quotient between the death threshold D_{death} and the division threshold P_{div}. A high value of $Q \in (0,1]$ corresponds to a cell that can cope with large proportions of damage before undergoing cell death and a small value correspond to a cell that can cope with small proportions of damage before cell death occurs.
$s \in \left[\frac{1}{2}, 1\right)$	The size proportion of the daughter and mother cell with respect to the original cell. The value $s = \frac{1}{2}$ corresponds to symmetric cell division and the value $s > \frac{1}{2}$ corresponds to asymmetric cell division.
$\text{re} \in [0,1]$	The retention parameter corresponding to the proportion of damage being retained in the mother cell after cell division. The value $\text{re} = 1$ corresponds to all damage being retained and the value $\text{re} = 0$ corresponds to no damage being retained.

The triangle of ageing

In order to pick biologically relevant parameter pairs (k_1, k_2), two conditions are imposed on the model. (1) Given enough food in the system, the cells should grow and as a consequence of cell growth damage is accumulated within the cell [34]. (2) Every cell within the population has a *finite* replicative life span implying that it should divide at least once and die after a finite number of cell divisions [4].

The first condition implies that both states P and D should be increasing functions of time and this is ensured by using linear stability analysis of the steady states. The second condition requires the derivation of the *lethal initial damage threshold* D_T. It corresponds to the critical damage proportion that a cell can obtain after cell division that inevitably leads to cell death. In other words, a cell obtaining more damage than D_T after cell division will undergo cell death while if it inherits less than this threshold value it will undergo at least one more cell division. A set of rate parameters (k_1, k_2) that allows for a finite RLS satisfies conditions based on two extreme cases determined by D_T. Firstly, with the given rate parameters the daughter cell with maximal fitness should divide at least once, and, secondly, the mother cell with a minimal fitness should undergo cell death. The initial lethal damage threshold is calculated by approximating trajectories of the solutions to the ODEs (Eq (4)) using piecewise linear approximations (See Supplementary Material S2.4). Using the above approach it is possible to define the conditions that allow for replicative ageing.

The outcome of the described analysis is the *triangle of ageing* (Fig 2A). This theoretical framework classifies all possible types of dynamics for any cell in the model into four categories: *starvation*, *immortality*, *ageing*, and *clonal senescence*. This implies that the parameter space is divided into four regions constrained by the *starvation*, *immortality* and *clonal senescence* constraints.

The *starvation constraint* predicts the minimum amount of substrate required for ageing (Eq (6)). Cells with parameters within the starvation region will not be able to form sufficient amounts of proteins leading to a collapse of the cellular machinery. The starvation constraint connects the uptake of nutrients to the damage accumulation process by acting as an upper bound on the sum of the damage formation and repair rates. The critical amount of substrate necessary for an organism to undergo ageing is $S_{\min} = \left(\frac{k_1+k_2}{g-(k_1+k_2)}\right) K_S$ in the case of Monod growth and if this constraint is not satisfied the cell will undergo starvation.

$$k_1 + k_2 < \mu(S) \cdot g \tag{6}$$

Cells that do not satisfy the *immortality constraint* have an infinite RLS (Eq (7)). It constitutes a lower bound on the damage formation rate or equivalently an upper bound on the damage repair rate and it is based on the value of D_T for the mother cell with minimal fitness. In other words, the constraint implies that the mother cell with minimal fitness with the given parameters (k_1, k_2) should undergo cell death.

$$D_T(k_1, k_2)|_{P=(s-\mathrm{re}(1-s)Q)} < (s + (1-s)\mathrm{re}) \tag{7}$$

Cells that do not satisfy the *clonal senescence constraint* have a RLS of zero divisions implying that they do not divide before undergoing cell death (Eq (8)). It acts as an upper bound on the damage formation rate or a lower bound on the repair rate and it is based on the value of D_T for the daughter cell with maximal fitness. In other words, the constraint implies that the daughter cell with maximal fitness with the given parameters (k_1, k_2) should divide.

$$D_T(k_1, k_2)|_{P=(1-s)} > 0 \tag{8}$$

The parameters that satisfy the starvation, immortality and clonal senescence constraints define the triangle of ageing. Within this triangle the RLS of an individual cell is inversely proportional to its rate of damage formation and proportional to its rate of repair which enables the construction of strategies for prolonging the RLS.

Two strategies for increasing the RLS: enhancing repair and slowing formation of damage

Next, we investigate the effect of the model parameters on the RLS of individual cells. In the triangle of ageing, the RLS can be increased by two obvious strategies: by decreasing the damage formation rate k_1 (Fig 2B) and by increasing the damage repair rate k_2 (Fig 2C). Here, we present the dynamics of the intact and damaged proteins for eight different damage-free daughters to verify the validity of the parameter constraints (Eq (6), (7) and (8)), and to elucidate the effect of altering the rate parameters according to the two proposed life prolonging strategies (Fig 2).

Figure 2. The triangle of ageing. **(A)** The constraints (Eq (6), (7) and (8)) on the rate of damage formation k_1 and repair k_2 define four different modes: *Starvation*, *Immortality*, *Clonal senescence* and *Ageing*. Cells with parameters above the dashed line will consume substrate too quickly and thereby undergo Starvation. Below the dashed line the parameters correspond to three types of cells characterised by Immortality (infinite RLS), Ageing (finite RLS) and Clonal Senescence (no RLS). Within the ageing region of the parameter space called *the triangle of ageing* the replicative life span (RLS) corresponding to a set of parameters is presented in the colour bar. (**B** & **C**) The formation of intact proteins P and damage D is simulated over time τ until cell death occurs. The threshold value determines when cell division ($P = 1$) or cell death ($D = 1$) occurs. **(B)** *Decreasing the formation of damage increases the RLS* ($k_1 \in \{0.22,\ 0.132,\ 0.1,\ 0.068,\ 0.04\}$ and fixed repair rate $k_2 = 0.15$). **(C)** *Increasing the repair rate increases the RLS* ($k_2 \in \{0.118,\ 0.15,\ 0.182,\ 0.32\}$ and fixed damage formation rate $k_1 = 0.1$). The other parameters used in the simulations are $\mu(S) = 0.6$, $g = 1.4$, $Q = {}^1/_3$, $s = {}^3/_4$, $(P_0, D_0) = (1 - s, 0)$ and $\mathrm{re} = 0.875$.

The results of the simulations confirm that a decrease in the formation of damage drastically affects the RLS of a single cell (Fig 2B). Similarly, an increase in the repair efficiency increases the RLS as well (Fig 2C) although the change is negligible compared to that of the other strategy. In addition, for the specific cell with $(k_1, k_2) = (0.1, 0.15)$ located within the triangle of ageing, a small decrease in the damage formation rate ($\Delta = 0.032$) increases the RLS with 18 divisions while the same increase in the repair rate yields a corresponding increase of only 1 division. This implies that the former strategy is more effective compared to the latter for the given set of parameters. Next, we set out to establish in a systematic manner whether or not this conclusion holds true for a large set of model parameters.

The retention mechanism is fundamental for replicative ageing

The strategies for prolonging the RLS are generalised in two steps. Firstly, the effect of retention on the two strategies is added to the analysis and secondly, the gains in RLS from the two strategies are compared for numerous cells with different capacity to retain damage. In our model, the distribution of damage depends on both the cell size and the damage retention parameter. Therefore, the triangle of ageing is generated for no ($\mathrm{re} = 0$, effectively the mother retains 75% of the existing damage), medium ($\mathrm{re} = 0.5$, effectively

the mother retains 87.5% of the existing damage) and high (re = 0.875, effectively the mother retains 96.9% of the existing damage) retention [8]. The results show that the ageing area of the parameter space increases with retention at the expense of the immortality region (Fig 3A). Thereby, cells with a functioning retention mechanism undergo ageing at lower rates of formation of damage. In addition, the relation between the area of the triangle of ageing and retention of damage indicates that the retention mechanism is tightly linked to ageing. Besides, a high degree of retention increases the set of parameters yielding a high RLS within the triangle of ageing implying that retention is also fundamental for longevity.

Next, we compare the two strategies for increasing the RLS of single cells accounting for retention (Fig 3B). For the same three retention profiles, the life spans of numerous damage-free daughter cells with equidistant parameters are simulated within the corresponding triangles of ageing. Thereafter the gain in RLS by decreasing the formation of damage given by $\Delta\mathrm{RLS}_{k_1} = \mathrm{RLS}\,(k_1 - \Delta_k, k_2) - \mathrm{RLS}\,(k_1, k_2)$ is compared to the gain in increasing the repair given by $\Delta\mathrm{RLS}_{k_2} = \mathrm{RLS}\,(k_1, k_2 + \Delta_k) - \mathrm{RLS}\,(k_1, k_2)$. Provided these values, all parameters for the three retention profiles are divided into three categories: *increasing the rate of repair* ''$\uparrow k_2$" where $\Delta\mathrm{RLS}_{k_1} < \Delta\mathrm{RLS}_{k_2}$, *decreasing the formation of damage* ''$\downarrow k_1$" where $\Delta\mathrm{RLS}_{k_1} > \Delta\mathrm{RLS}_{k_2}$ and the *neutral strategy* ''neutral" where $\Delta\mathrm{RLS}_{k_1} = \Delta\mathrm{RLS}_{k_2}$ (Fig 3B).

Figure 3. Retention is crucial for replicative ageing.(**A**) The effect of retention on the triangle of ageing. The triangles of ageing are generated for three retention profiles (from the left column to the right: none re = 0, medium re = 0.5 and high re = 0.875). The area of the ageing region increases to the left at the expense of the immortality region proportionally to the degree of retention of damage. (**B**) The efficiency of the RLS prolonging strategies as a function of retention. The increases in RLS of single cells by increasing the repair rate and decreasing the formation of damage are compared for the same three retention profiles as in (A). The cells are divided into three categories: Orange (''$\downarrow k_1$"): *decrease in formation of damage* where $\Delta\mathrm{RLS}_{k_1} > \Delta\mathrm{RLS}_{k_2}$, Green (''$\uparrow k_2$"): *increase in rate of repair* where $\Delta\mathrm{RLS}_{k_1} < \Delta\mathrm{RLS}_{k_2}$ and Grey (''neutral"): *both strategies* are equally good where $\Delta\mathrm{RLS}_{k_1} = \Delta\mathrm{RLS}_{k_2}$. The other parameter used in the simulations are $\mu(S) = 0.6$, $g = 1.4$, $Q = {}^1/_3$, $s = {}^3/_4$ and $(P_0, D_0) = (1 - s, 0)$.

We found that for 60 to 80% of the cells independent of retention profile, both strategies are equally effective in increasing the RLS (Fig 3B). Accordingly, the formation and repair of damage are fundamental to the accumulation of damage. Therefore, a profound understanding of these forces is required in order to fully grasp the mechanisms behind replicative ageing. Moreover, the retention mechanism increases the importance of an effective repair machinery since the number of cells for which a decrease in formation of damage is favourable is reduced (a decrease from ca 30 to 15%) and the number of cells for which both strategies are effective is increased (an increase from ca 65 to 80%) as retention is introduced. This finding suggests that the cellular machinery responsible for retention and repair of damage are interlinked which is confirmed by earlier experimental studies [24].

Long lived yeast strains with a functioning retention mechanism have an effective repair machinery

The model is validated by a published data-set consisting of strain-specific distributions of the RLS and mean generation times [35]. Using a microfluidics system, Liu and

Acar obtained experimental data for 200 individual yeast cells from the short-lived *sir2*Δ, the wild type *wt*, and the long-lived *fob1*Δ strain [35]. In this study, normal distributions were fitted to the RLSs of the populations from the three strains and the mean generation times of the same strains were fitted to a power law (Supplementary material S1.1). Given these RLS distributions and the mean generation times, the model is calibrated with respect to these two metrics for the three strains by using a parameter estimation procedure (see Supplementary material S3.4). As the *wt* and *fob1*Δ strains have a functioning retention machinery, the selection of parameters for these strains is implemented with the retention value re $= 0.875$. However, it is well-established that the Sir2p is crucial in order for the ageing mother cell to properly retain damage [3, 36, 37] and therefore the value re $= 0$ is implemented for the *sir2*Δ strain (Fig 4).

Figure 4. Model validation using RLS data. The RLS distributions (**A**) and mean generation times (**B**) for populations of cells from three different yeast strains: the short lived *sir2*Δ (left column), the wild type *wt* (middle column) and the long lived *fob1*Δ (right column). Colour coding: the blue histograms and the blue curves correspond to the simulated output while the red counterparts correspond to the experimentally measured data. The data for the RLS distributions is generated by plotting the density function of the normal distribution multiplied by the number of cells in the population.

Qualitatively, these results indicate that the constructed model of accumulation of damage is capable of describing replicative ageing in yeast. The model with the fitted parameters captures the mean value with high precision and the increase in generation times reasonably well indicating that the underlying assumptions behind the model are valid. However, for all three strains, the model cannot capture the standard deviation in RLS (only between 20 to 25% of the spread in the RLS distributions is captured) which can be explained by the fact that the model focuses merely on the accumulation of damaged proteins. Nevertheless, as there are multiple *ageing factors* such as extrachromosomal rDNA circles (ERCs), reactive oxygen species or DNA mutations that influence the RLS of *S.cerevisiae* [38] it is reasonable to assume that these factors account for a portion of the spread in the RLS distribution which cannot be accounted for by our model. For example, it has been shown that the *sir2*Δ-strain has both elevated ERC-levels and a dysfunctional retention machinery [39], whereas the *fob1*Δ-strain has reduced ERC levels [40].

Table 2. Parameters for the three yeast strains. In the three columns from left to right: yeast strain, parameters and the output. The remaining parameters are $\mu = 0.6$, $Q = {}^1/_3$, $s = {}^3/_4$ and $(P_0, D_0) = (1 - s, 0)$

Strain (μ, σ)	**Parameters** $(g, \overline{k}_1, \overline{k}_2, \sigma_k, \mathrm{re})$	**Output** $(\overline{RLS}, \sigma_{\mathrm{RLS}})$
*sir2*Δ $(14.00, 4.80)$	$(1.4, 0.1160, 0.0600, 0.009, 0)$	$(14.06, 1.08)$
wt $(23.5, 8.1)$	$(1.4, 0.0628, 0.1300, 0.0125, 0.875)$	$(22.37, 1.82)$
*fob1*Δ $(31.9, 11.8)$	$(1.7, 0.0715, 0.1400, 0.009, 0.875)$	$(31.39, 2.54)$

Furthermore, the results of the parameter estimation confirm the connection between the retention and repair of damage. This can be seen by comparing the magnitudes of the formation and repair of damage between the *wt* and *fob1*Δ strains with retention on the one hand, and the *sir*2Δ strain without retention on the other. The short lived strain has a substantially higher damage formation rate k_1 than repair rate k_2 while the reverse relation holds true for the two long lived strains (Tab 2). Consequently, this result reaffirms the connection between the retention machinery and the capacity to repair damage. Nevertheless, it should be emphasised that the fitted parameters are not unique entailing that there are numerous local optimal sets of parameters within the triangle of ageing that can be selected based on the data. Despite of the parameter estimation problem being ill-posed, the conclusion regarding the connection between repair and retention of damage is still valid. As the interesting parameters corresponding to a high RLS are located close to the immortality region (Fig 3A), it is clear that the damage formation rate k_1 is much lower for cells with retention than without. This implies that the former category of cells will have a higher repair rate k_2 *in relation* to its damage formation rate than the latter.

Moreover, experimental studies have shown that *sir2*Δ mutants divide more symmetrically compared to wild type cells [41] suggesting that asymmetry is coupled with retention of damage. We have shown the essential role that retention of damage plays in the ageing process and accordingly the link between asymmetry and retention suggests that asymmetric division is beneficial in the context of unicellular ageing. Therefore, we subsequently asked what roles asymmetry and resilience to damage play in the replicative ageing process.

The triangle of ageing reveals the benefit of asymmetric cell division and high resilience in relation to longevity

We evaluate the significance of asymmetric division and resilience to damage by perturbing the triangle of ageing. Given a set of parameters, four different triangles are generated for low ($Q = {}^1/_3$) and high ($Q = {}^1/_2$) resilience to damage as well as for symmetric ($s = {}^1/_2$) and asymmetric ($s = {}^3/_4$) cell division (Fig 5). An increase in resilience

to damage shifts the triangle of ageing to the right implying that resilient organisms undergo ageing at high rates of formation of damage. The effect of an increased resilience is that the RLS of a cell is prolonged since the immortality region moves closer to the corresponding point in the parameter space as the value of Q increases. This confirms the previous simulations (Fig 1C).

Similarly, a higher degree of asymmetry in the cell division yields a longer life span. Within the triangles of ageing, the RLS is higher in the asymmetric (bottom row of Fig 5) compared to the symmetric (top row of Fig 5) case giving weight to the proposed link between asymmetric cell division and longevity in the context of replicative ageing. This is supported by the comparison between stem cells for which the asymmetric cell division results in a rejuvenated daughter cell and symmetrically dividing neurons where the amount of damage is greater due to the incapacity to remove damage through cell division [42].

Figure 5. The benefit of asymmetric cell division and a high resilience to damage in the context of ageing. Four triangles of ageing are generated for two levels of resilience to damage ($Q = {}^1/_3$ left column & $Q = {}^1/_2$ right column) and two different size proportions in the cell division (symmetric $s = {}^1/_2$ top row & $s = {}^3/_4$ bottom row). The other parameters used for generating the triangles are $\mu = 0.6$, $g = 1.4$ and $\mathrm{re} = 0.875$.

Discussion & Conclusions

To achieve a successful extension of the RLS of a single cell, the interplay between the formation, repair and distribution of damage upon cell division is vital. In this study, a comprehensive theoretical description of the accumulation of damaged proteins is presented resulting in four main findings. (I): A mathematical model of the replicative ageing of single cells accounting for all key properties which forms the basis for the *triangle of ageing* (Fig 2A). The latter framework states which of the modes starvation, immortality, clonal senescence, or ageing a cell will undergo in terms of the forces cell growth, formation of damage, repair of damage, cell division and cell death. (II): Three strategies for increasing the RLS of an individual cell, namely decreasing the damage formation rate (Fig 2B), increasing the repair rate (Fig 2C) and increasing the resilience to damage (Fig 1C). (III): The triangle of ageing indicates that retention of damage is closely connected to replicative ageing (Fig 3A). Further, retention increases the benefit of improving the capacity to repair damage in relation to extending the RLS (Fig 3B) and the model is in agreement with experimental data (Fig 4). The validation of the model suggests that both the wild type and the long-lived *fob1*Δ strains have low damage formation rates as well as efficient repair machineries on account of their functioning retention mechanisms (Tab 2). (IV): The model suggests that asymmetric cell division and replicative ageing are closely linked illustrated by perturbing the parameters in the triangle of ageing (Fig 5).

The presented model is novel in three respects: it links all major biological features of accumulation of damage, it focuses on replicative ageing and its methodology combines mathematical analysis with simulations. Using the triangle of ageing, we can confirm previous results such as showing the importance of repair [11], the critical role of asymmetric segregation of damage through retention in the context of ageing [12, 13] and that cells forming damage with a rate under a certain threshold result in immortal lineages [12]. In addition, using this framework we can also connect all key factors having profound implications on replicative ageing. Thereby, we enable the study of the relationships between the key properties of ageing as opposed to study them individually.

For example, the starvation constraint (Eq (6)) connects the uptake of food to the damage accumulation process. Moving forward, two main tasks ought to be tackled, namely to validate the model with time series data and to render the model more quantifiable. Within the triangle of ageing (Fig 1A), there exist multiple sets of parameters resulting in the same replicative life span. Consequently, using the data at hand consisting of RLS distributions and mean generation times it is not possible to identify both the damage formation rate k_1 and the repair rate k_2 as there are multiple local optimal parameter sets. In order to address the mentioned identifiability problem, the model could be validated using time series data of intracellular proteins or cell mass over time. Secondly, the quantifiability of the model can be increased by considering each of the key processes as modules. More precisely, by defining the modules cell growth, repair, formation, cell division and cell death it is possible to expand the level of detail in each module by studying specific intracellular pathways connected to these processes. Using the current model as interfaces between these modules it is possible to construct a quantitative model of replicative ageing in unicellular organisms like *S.cerevisiae*.

The RLS of an individual cell is highly dependent on the mechanisms behind damage formation, repair, resilience and retention. To increase the RLS, the strategies of enhancing the capacity to repair and decreasing formation of damage are proposed (Fig 2). Furthermore, as a consequence of the non-dimensionalisation procedure, the intrinsic property of resilience to damage Q emerges which is essential to the replicative ageing of a single cell where an increase in resilience greatly prolongs the life span (Fig 1C & 5). By understanding the biological properties that govern these forces it is possible to increase the replicative potential of an organism. Moreover, the results indicate that the repair of damage is coupled to the retention mechanism (Fig 3) as introducing retention increases the benefit of enhancing the repair machinery. Prioritising retention implies a high value of D after cell division resulting in a low cell growth term which in turn decreases the RLS. Therefore, a small increase in the rate parameter k_2 will increase the RLS for a cell with a functioning retention mechanism. Also, the results indicate that the retention mechanism is tightly coupled to replicative ageing (Fig 3A) reaffirming the importance of the budding event with respect to the ageing process in *S.cerevisiae*. In addition, the short-lived *sir2*Δ-strain with a malfunctioning retention mechanism has also an inefficient repair machinery compared to the longer lived strains (Tab 2). This reinforces the fact that repair and retention of damage are interlinked. Thus, in order to obtain a mechanistic understanding of the ageing process in somatic cells or eukaryotic organisms overall, it is critical to investigate the constituents of the retention machinery.

The triangle of ageing suggests that asymmetric division is beneficial in the context of replicative ageing (Fig 5). When comparing the effect of symmetric versus asymmetric cell division, our results indicate that the latter mode of division yields a higher RLS compared to the former. In order to ensure the viability of cell lines, the asymmetric segregation of damage at the point of cell division is crucial. This segregation is ensured by the retention mechanism but it has also been speculated that it is enhanced by asymmetric division. When comparing asymmetrically dividing stem cells with symmetrically dividing neurons the former class of cells is able to remove damage through cell division to a larger extent while the latter has a higher instance of damage inclusions [42]. In addition, the short-lived *sir2*Δ mutant of yeast divides more symmetrically [41] than the wild type counterpart indicating that asymmetric cell division benefits longevity.

Further, the triangle of ageing displays the link between cell growth and formation of damage. Under favourable conditions in terms of available substrate, it has been speculated that *E.coli* does not undergo replicative ageing [43, 44, 9] which entails that its parameters are located in the immortality region of the parameter space. Such parameters correspond to low rates of formation of damage which in turn corresponds to a high growth rate as $k_1 \propto \left({}^{1}/_{\mu_{\max}}\right)$ (Tab 1). Furthermore, the genome size of

E.coli is substantially smaller compared to that of *S.cerevisiae*, namely ∼4.64Mbp [45] versus ∼12.07Mbp [46]. Due to the small genome size, it is not required to spend large resources on the maintenance of the cell. From this follows that it is reasonable to assume that *E.coli* has a low rate of formation of damage. In accordance with the "Disposable Soma"-theory [47], this allows it to prioritise cell growth over maintenance, and thus a high rate of cell growth should be indicative of a low rate of damage formation which is what the triangle of ageing suggests. Besides, it has been shown that *E.coli* has optimised its metabolic flux to achieve a maximal growth rate [48]. This suggest that *E.coli* strongly favours growth, and therefore spends less energy on maintenance which results in it not undergoing ageing when growth conditions are optimal. Furthermore, Wasko et al. proposed that growth rate, rather than replicative lifespan, is a more appropriate measure of fecundity [49]. They argue that there is a minimal benefit of increasing the lifespan by one generation on the population level in contrast to the significant gain brought by a small increase in growth rate. These observations establish the close link between cell growth and formation of damage. This implies that rapidly growing organisms with small genomes do not undergo ageing under optimal conditions. On the other hand, slower growing organisms with larger genomes are forced to maintain their cell and therefore undergo replicative ageing as a by-product of growth. This balance between growth and maintenance of the cell is captured by the triangle of ageing. Thus our work raises the question if ageing is not a consequence of cell maintenance.

Materials and Methods

All the numerical results were generated using Matlab [50]. The system of ODEs (Eq (4)) has been solved using the built-in solver "ode45" which uses an adaptive "Runge-Kutta-Fehlberg"-method of order 4 and 5 [51]. In addition, the immortality and clonal senescence constraints (Eq (7) and (8)) in the triangle of ageing (Fig 2A) have been generated using an approximation procedure. This entails generating a piecewise linear approximation of the critical trajectory representing the lethal inital damage threshold D_T by approximating a solution to the system of ODEs using multiple lines. A detailed description of the numerical implementations of the algorithms used for generating the results can be found in the Appendix (See Supplementary material S3).

Supporting information

S1 Appendix. Supplementary material. The appendix contains the data, the parameter values used in the study, a detailed mathematical analysis and a description of the numerical implementations.

Acknowledgments

We would like to thank Qasim Ali, Annikka Polster, Felix Held and Barbara Schnitzer for valuable input and careful reading of the manuscript.

References

1. He C, Zhou C, Kennedy BK. The yeast replicative aging model. Biochimica et Biophysica Acta (BBA)-Molecular Basis of Disease. 2018;.

2. McCormick MA, Delaney JR, Tsuchiya M, Tsuchiyama S, Shemorry A, Sim S, et al. A comprehensive analysis of replicative lifespan in 4,698 single-gene deletion strains uncovers conserved mechanisms of aging. Cell metabolism. 2015;22(5):895–906.

3. Liu B, Larsson L, Caballero A, Hao X, Öling D, Grantham J, et al. The polarisome is required for segregation and retrograde transport of protein aggregates. Cell. 2010;140(2):257–267.

4. Mortimer RK, Johnston JR. Life span of individual yeast cells. 1958;.

5. Aguilaniu H, Gustafsson L, Rigoulet M, Nyström T. Asymmetric inheritance of oxidatively damaged proteins during cytokinesis. Science. 2003;299(5613):1751–1753.

6. Kirkwood TBL. Evolution of ageing. Nature. 1977;270:301–304.

7. Ackermann M, Chao L, Bergstrom CT, Doebeli M. On the evolutionary origin of aging. Aging cell. 2007;6(2):235–244.

8. Erjavec N, Cvijovic M, Klipp E, Nyström T. Selective benefits of damage partitioning in unicellular systems and its effects on aging. Proceedings of the National Academy of Sciences. 2008;105(48):18764–18769.

9. Chao L. A model for damage load and its implications for the evolution of bacterial aging. PLoS Genet. 2010;6(8):e1001076.

10. Rashidi A, Kirkwood TBL, Shanley DP. Evolution of Asymmetric Damage Segregation: A Modelling Approach. Aging Research in Yeast. 2012; p. 315.

11. Clegg RJ, Dyson RJ, Kreft JU. Repair rather than segregation of damage is the optimal unicellular aging strategy. BMC biology. 2014;12(1):1.

12. Chao L, Rang CU, Proenca AM, Chao JU. Asymmetrical Damage Partitioning in Bacteria: A Model for the Evolution of Stochasticity, Determinism, and Genetic Assimilation. PLoS Comput Biol. 2016;12(1):e1004700.

13. Vedel S, Nunns H, Košmrlj A, Semsey S, Trusina A. Asymmetric damage segregation constitutes an emergent population-level stress response. Cell systems. 2016;3(2):187–198.

14. Chen KL, Crane MM, Kaeberlein M. Microfluidic technologies for yeast replicative lifespan studies. Mechanisms of ageing and development. 2017;161:262–269.

15. Broach JR. Nutritional control of growth and development in yeast. Genetics. 2012;192(1):73–105. doi:10.1534/genetics.111.135731.

16. Snoep JL, Mrwebi M, Schuurmans JM, Rohwer JM, de Mattos MJT. Control of specific growth rate in Saccharomyces cerevisiae. Microbiology. 2009;155(5):1699–1707.

17. Lee SS, Vizcarra IA, Huberts DH, Lee LP, Heinemann M. Whole lifespan microscopic observation of budding yeast aging through a microfluidic dissection platform. Proceedings of the National Academy of Sciences. 2012; p. 201113505.

18. Jo MC, Liu W, Gu L, Dang W, Qin L. High-throughput analysis of yeast replicative aging using a microfluidic system. Proceedings of the National Academy of Sciences. 2015;112(30):9364–9369.

19. Lindner AB, Madden R, Demarez A, Stewart EJ, Taddei F. Asymmetric segregation of protein aggregates is associated with cellular aging and rejuvenation. Proceedings of the National Academy of Sciences of the United States of America. 2008;105(8):3076–3081. doi:10.1073/pnas.0708931105.

20. Higuchi-Sanabria R, Pernice WMA, Vevea JD, Alessi Wolken DM, Boldogh IR, Pon LA. Role of asymmetric cell division in lifespan control in Saccharomyces cerevisiae. FEMS yeast research. 2014;14(8):1133–1146. doi:10.1111/1567-1364.12216.

21. Nystrom T, Liu B. The mystery of aging and rejuvenation - a budding topic. Current opinion in microbiology. 2014;18:61–67. doi:10.1016/j.mib.2014.02.003.

22. Henderson KA, Gottschling DE. A mother's sacrifice: what is she keeping for herself? Current opinion in cell biology. 2008;20(6):723–728.

23. Amm I, Sommer T, Wolf DH. Protein quality control and elimination of protein waste: the role of the ubiquitin-proteasome system. Biochimica et biophysica acta. 2014;1843(1):182–196. doi:10.1016/j.bbamcr.2013.06.031.

24. Nyström T, Liu B. Protein quality control in time and space–links to cellular aging. FEMS yeast research. 2014;14(1):40–48.

25. Hill SM, Hao X, Grönvall J, Spikings-Nordby S, Widlund PO, Amen T, et al. Asymmetric inheritance of aggregated proteins and age reset in yeast are regulated by Vac17-dependent vacuolar functions. Cell reports. 2016;16(3):826–838.

26. Warner HR, Hodes RJ, Pocinki K. What does cell death have to do with aging? Journal of the American Geriatrics Society. 1997;45(9):1140–1146.

27. Laun P, Pichova A, Madeo F, Fuchs J, Ellinger A, Kohlwein S, et al. Aged mother cells of Saccharomyces cerevisiae show markers of oxidative stress and apoptosis. Molecular microbiology. 2001;39(5):1166–1173.

28. Falcone C, Mazzoni C. External and internal triggers of cell death in yeast. Cellular and Molecular Life Sciences. 2016;73:2237–2250. doi:10.1007/s00018-016-2197-y.

29. Woldringh CL, Huls PG, Vischer NO. Volume growth of daughter and parent cells during the cell cycle of Saccharomyces cerevisiae a/alpha as determined by image cytometry. Journal of bacteriology. 1993;175(10):3174–3181.

30. Limpert E, Stahel WA, Abbt M. Log-normal Distributions across the Sciences: Keys and Clues: On the charms of statistics, and how mechanical models resembling gambling machines offer a link to a handy way to characterize log-normal distributions, which can provide deeper insight into v. AIBS Bulletin. 2001;51(5):341–352.

31. Limpert E, Stahel WA. Problems with using the normal distribution–and ways to improve quality and efficiency of data analysis. PLoS One. 2011;6(7):e21403.

32. Almquist J, Bendrioua L, Adiels CB, Goksör M, Hohmann S, Jirstrand M. A nonlinear mixed effects approach for modeling the cell-to-cell variability of Mig1 dynamics in yeast. PloS one. 2015;10(4):e0124050.

33. Welkenhuysen N, Borgqvist J, Backman M, Bendrioua L, Goksör M, Adiels CB, et al. Single-cell study links metabolism with nutrient signaling and reveals sources of variability. BMC Systems Biology. 2017;11(1). doi:10.1186/s12918-017-0435-z.

34. Egilmez NK, Jazwinski SM. Evidence for the involvement of a cytoplasmic factor in the aging of the yeast Saccharomyces cerevisiae. Journal of bacteriology. 1989;171(1):37–42.

35. Liu P, Acar M. The generational scalability of single-cell replicative aging. Science advances. 2018;4(1):eaao4666.

36. Erjavec N, Nyström T. Sir2p-dependent protein segregation gives rise to a superior reactive oxygen species management in the progeny of Saccharomyces cerevisiae. Proceedings of the National Academy of Sciences. 2007;104(26):10877–10881.

37. Nyström T. Spatial protein quality control and the evolution of lineage-specific ageing. Philosophical Transactions of the Royal Society of London B: Biological Sciences. 2011;366(1561):71–75.

38. Denoth Lippuner A, Julou T, Barral Y. Budding yeast as a model organism to study the effects of age. FEMS microbiology reviews. 2014;38(2):300–325.

39. Erjavec N, Larsson L, Grantham J, Nyström T. Accelerated aging and failure to segregate damaged proteins in Sir2 mutants can be suppressed by overproducing the protein aggregation-remodeling factor Hsp104p. Genes & development. 2007;21(19):2410–2421.

40. Kaeberlein M, McVey M, Guarente L. The SIR2/3/4 complex and SIR2 alone promote longevity in Saccharomyces cerevisiae by two different mechanisms. Genes & development. 1999;13(19):2570–2580.

41. Song J, Yang Q, Yang J, Larsson L, Hao X, Zhu X, et al. Essential genetic interactors of SIR2 required for spatial sequestration and asymmetrical inheritance of protein aggregates. PLoS genetics. 2014;10(7):e1004539.

42. Schneider KL, Nyström T, Widlund PO. Studying spatial protein quality control, proteopathies, and aging using different model misfolding proteins in S. cerevisiae. Frontiers in molecular neuroscience. 2018;11:249.

43. Wang P, Robert L, Pelletier J, Dang WL, Taddei F, Wright A, et al. Robust growth of Escherichia coli. Current biology. 2010;20(12):1099–1103.

44. Florea M. Aging and immortality in unicellular species. Mechanisms of ageing and development. 2017;167:5–15.

45. Blattner FR, Plunkett G, Bloch CA, Perna NT, Burland V, Riley M, et al. The complete genome sequence of Escherichia coli K-12. science. 1997;277(5331):1453–1462.

46. Valle D. Life with 6000 Genes A. Goffeau,* BG Barrell, H. Bussey, RW Davis, B. Dujon, H. Feldmann, F. Galibert, JD Hoheisel, C. Jacq, M. Johnston, E. J. Louis, HW Mewes, Y. Murakami, P. Philippsen, H. Tettelin, SG Oliver. Methods Enzymol. 1996;266:141.

47. Kirkwood TBL, Austad SN. Why do we age? Nature. 2000;408(6809):233–238.

48. Edwards JS, Ibarra RU, Palsson BO. In silico predictions of Escherichia coli metabolic capabilities are consistent with experimental data. Nature biotechnology. 2001;19(2):125.

49. Wasko BM, Kaeberlein M. Yeast replicative aging: a paradigm for defining conserved longevity interventions. FEMS yeast research. 2014;14(1):148–159.

50. MATLAB. version 9.4.0.813654 (R2018a). Natick, Massachusetts: The MathWorks Inc.; 2018.

51. Cheney W, Kincaid D. Numerical Mathematics and Computing. 7th ed. Brooks/-Cole Cengage Learning; 2013.

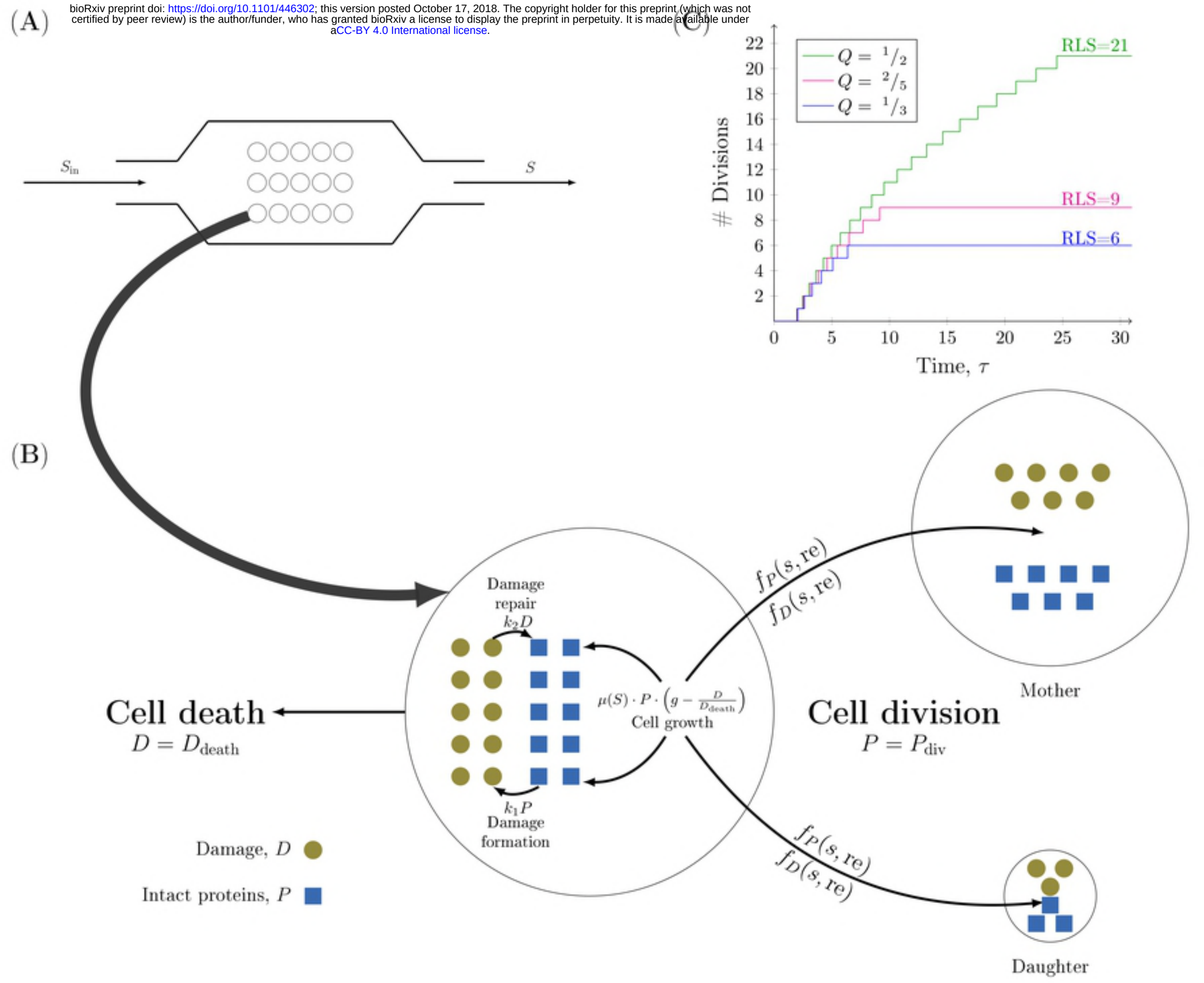

Figure 1

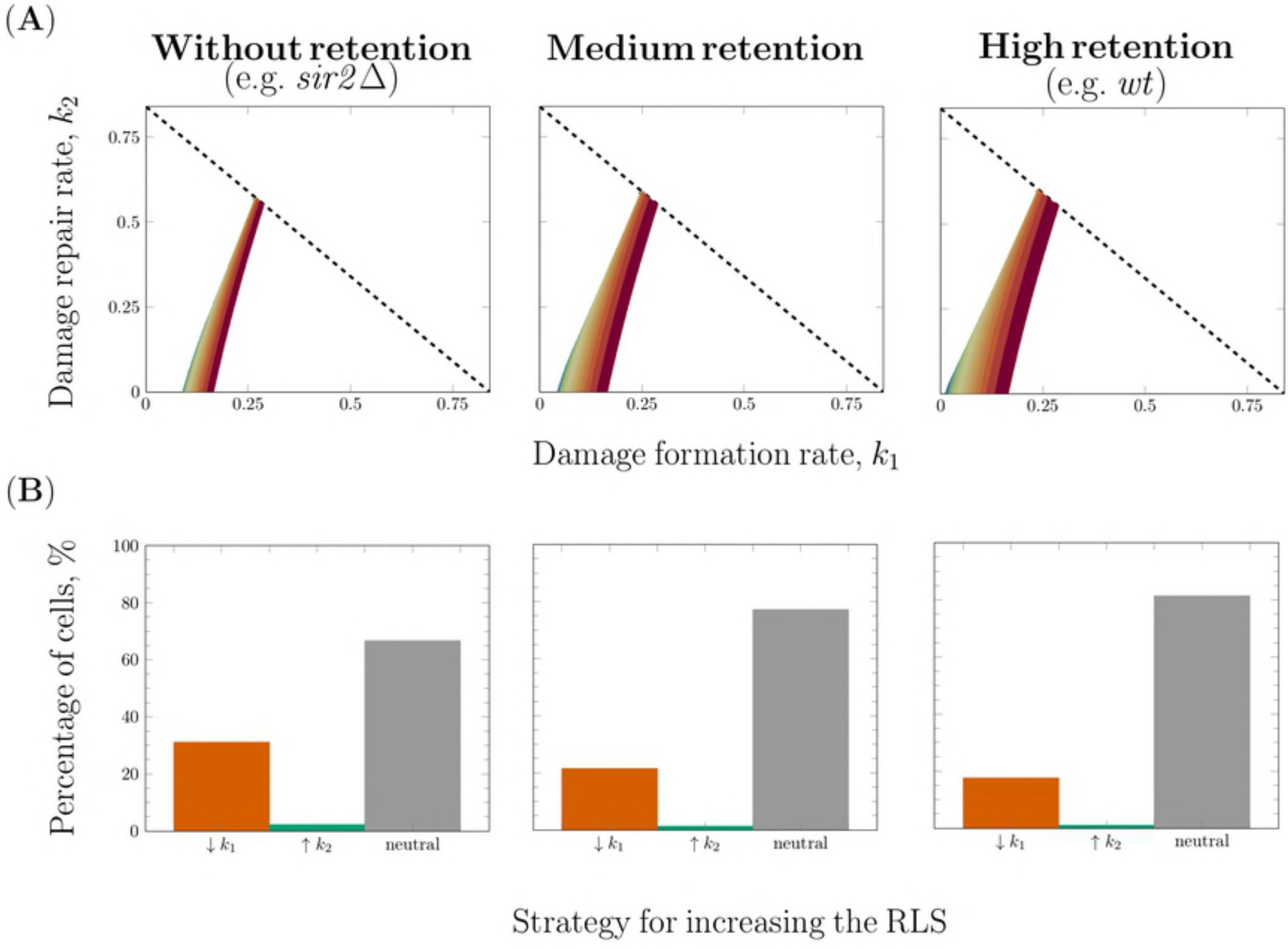
(A)
Without retention
(e.g. sir2Δ)
Medium retention
High retention
(e.g. wt)
Damage repair rate, k_2
0.75
0.5
0.25
0
0
0.25
0.5
0.75
Damage formation rate, k_1
(B)
Percentage of cells, %
100
80
60
40
20
0
$\downarrow k_1$
$\uparrow k_2$
neutral
Strategy for increasing the RLS

Figure 3

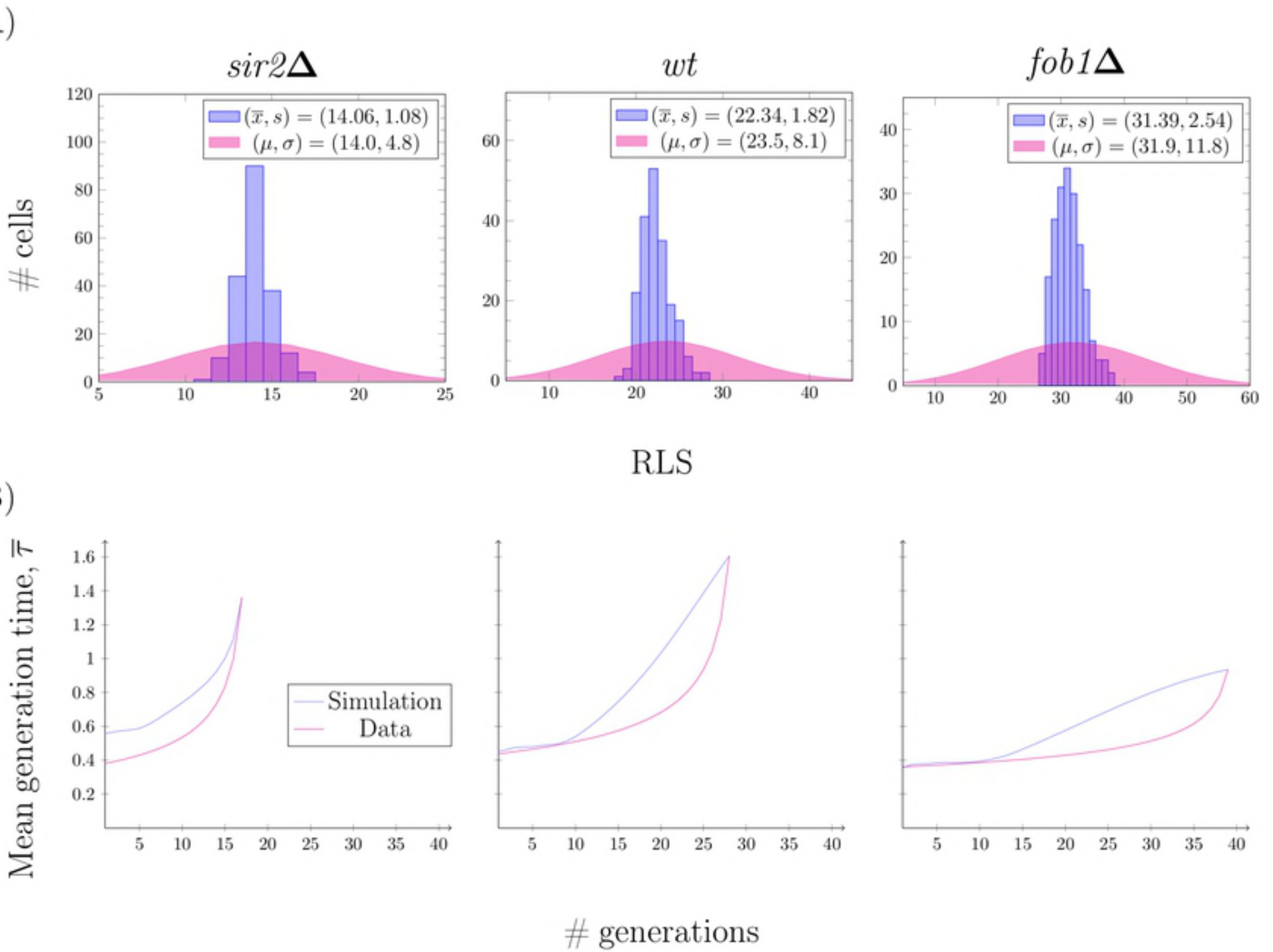
(A)
sir2Δ
wt
fob1Δ
cells
$(\overline{x}, s) = (14.06, 1.08)$
$(\mu, \sigma) = (14.0, 4.8)$
$(\overline{x}, s) = (22.34, 1.82)$
$(\mu, \sigma) = (23.5, 8.1)$
$(\overline{x}, s) = (31.39, 2.54)$
$(\mu, \sigma) = (31.9, 11.8)$
RLS
(B)
Mean generation time, $\overline{\tau}$
Simulation
Data
generations

Figure 4

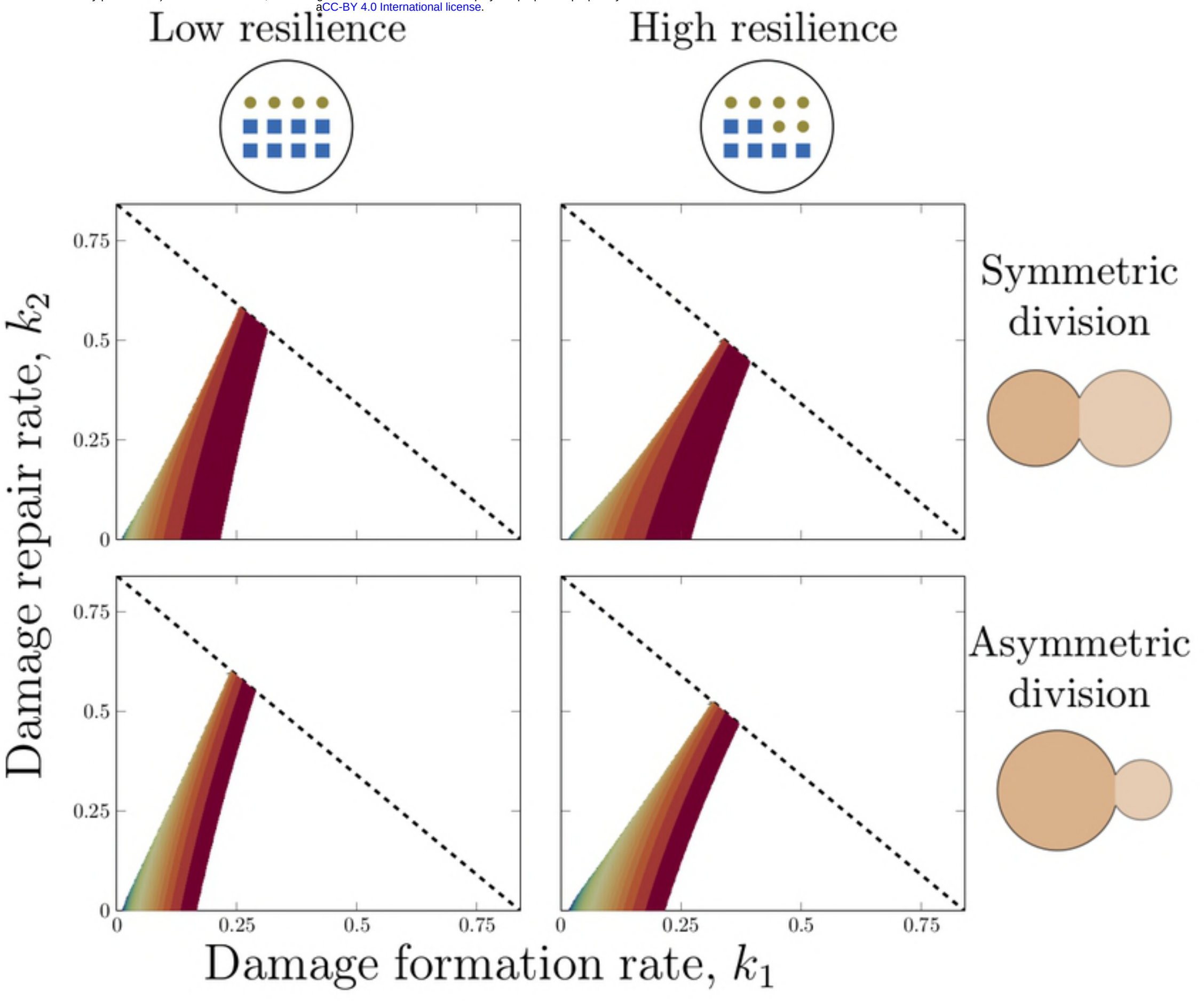

Figure 5

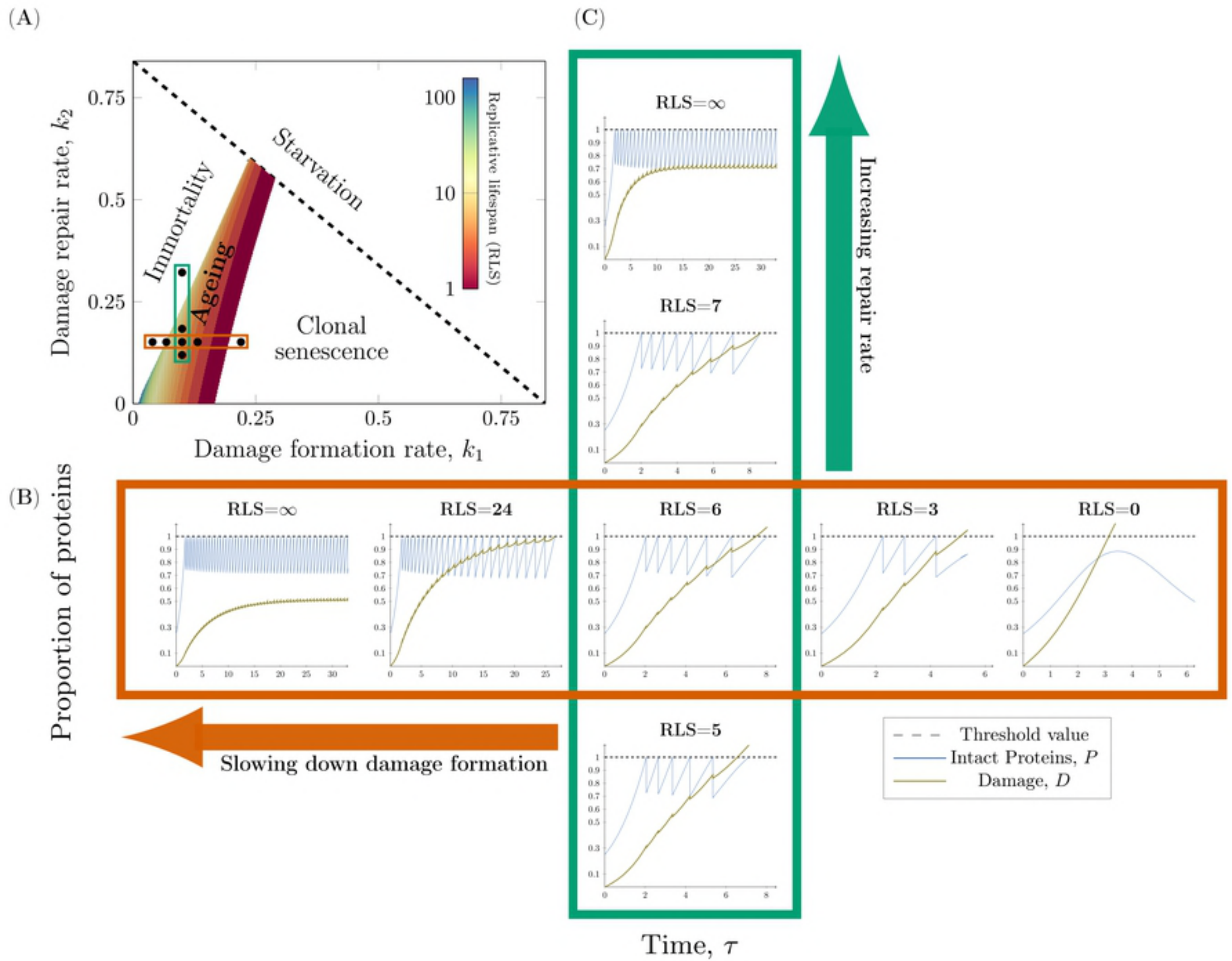
(A)
Damage repair rate, k_2
Damage formation rate, k_1
Immortality
Ageing
Starvation
Clonal senescence
Replicative lifespan (RLS)
100
10
1
(B)
Proportion of proteins
RLS=∞
RLS=24
RLS=6
RLS=3
RLS=0
RLS=5
Slowing down damage formation
Time, τ
(C)
RLS=∞
RLS=7
Increasing repair rate
Threshold value
Intact Proteins, P
Damage, D

FIgure 2